Structural Determinants of Slow Inactivation in Human Cardiac and Skeletal Muscle Sodium Channels

Yuriy Y. Vilin,* Naomasa Makita,# Alfred L. George, Jr.,§ and Peter C. Ruben*

*Department of Biology, Utah State University, Logan, Utah 84322 USA; #Department of Cardiovascular Medicine, Hokkaido University School of Medicine, Sapporo, Japan; and §Departments of Medicine and Pharmacology, Vanderbilt University, Nashville, Tennessee 37232 USA

ABSTRACT Skeletal and heart muscle excitability is based upon the pool of available sodium channels as determined by both fast and slow inactivation. Slow inactivation in hH1 sodium channels significantly differs from slow inactivation in hSkM1. The β_1-subunit modulates fast inactivation in human skeletal sodium channels (hSkM1) but has little effect on fast inactivation in human cardiac sodium channels (hH1). The role of the β_1-subunit in sodium channel slow inactivation is still unknown. We used the macropatch technique on *Xenopus* oocytes to study hSkM1 and hH1 slow inactivation with and without β_1-subunit coexpression. Our results indicate that the β_1-subunit is partly responsible for differences in steady-state slow inactivation between hSkM1 and hH1 channels. We also studied a sodium channel chimera, in which P-loops from each domain in hSkM1 sodium channels were replaced with corresponding regions from hH1. Our results show that these chimeras exhibit hH1-like properties of steady-state slow inactivation. These data suggest that P-loops are structural determinants of sodium channel slow inactivation, and that the β_1-subunit modulates slow inactivation in hSkM1 but not hH1. Changes in slow inactivation time constants in sodium channels coexpressed with the β_1-subunit indicate possible interactions among the β_1-subunit, P-loops, and the slow inactivation gate in sodium channels.

INTRODUCTION

Slow inactivation in voltage-gated sodium channels is a biophysical process that plays an important role in membrane excitability and firing properties (Ruff et al., 1988; Sawczuk et al., 1995; Fleidervish et al., 1996). Discovered almost three decades ago (Chandler and Meves, 1970; Rudy, 1978), slow inactivation has recently attracted attention because of its unusual properties, its physiological importance, and its unclear molecular basis. Slow inactivation is a process that is different from fast inactivation in Na^+ channels as described by Hodgkin and Huxley (1952). Removal of fast inactivation with pronase (Rudy, 1978), trypsin (Starkus and Shrager, 1978), α-chymotrypsin (Valenzuela and Bennett, 1994), or *N*-bromoacetamide (Salgado et al., 1985) has no effect on slow inactivation. Fast inactivation and slow inactivation are also kinetically different. Fast inactivation occurs within milliseconds (Hille, 1992), and slow inactivation develops on the order of seconds (Ruff et al., 1988; Wang and Wang, 1997). Mutating the IFM fast inactivation gating particle in the DIII-IV linker to QQQ completely removes fast inactivation (West et al., 1992) but leaves slow inactivation intact (Featherstone et al., 1996). Slow inactivation does not affect recovery from fast inactivation in rSkM1 channels expressed in *Xenopus* oocytes (Vedantham and Cannon, 1998). These data suggest that the structural basis for slow inactivation gating is different from gating of fast inactivation.

Received for publication 8 April 1999 and in final form 16 June 1999.

Address reprint requests to Dr. Peter C. Ruben, Department of Biology, Utah State University, Logan, UT 84322. Tel.: 435-797-2490; Fax: 435-797-1575; E-mail: pruben@biology.usu.edu.

0006-3495/99/09/1384/10 $2.00

Mutations that change sodium channel slow inactivation may lead to serious diseases. For example, alterations in slow inactivation of human skeletal muscle sodium channels lead to hyperkalemic periodic paralysis (Cummins and Sigworth, 1996; Hayward et al., 1997, 1999).

Slow inactivation differs between human skeletal muscle sodium channels (hSkM1) and human heart sodium channels (hH1). Recent studies have shown that steady-state slow inactivation is only ~40% complete in hH1 sodium channels, compared to ~80% in hSkM1 sodium channels expressed in *Xenopus* oocytes (Richmond et al., 1998) or human embryonic kidney cells (O'Reilly et al., 1999). There are at least two possible reasons for these observations. The molecular structure of the hSkM1 α-subunit differs from that of the hH1 α-subunit (Trimmer et al., 1989; George et al., 1992; Rogart et al., 1989; Gellens et al., 1992). Furthermore, hSkM1 and brain sodium channels require coexpression of β_1 subunit for normal gating (Isom et al., 1992; Cannon et al., 1993; Yang et al., 1993; Patton et al., 1994). In contrast, β_1 coexpression is not required for normal gating characteristics of hH1 channels expressed in oocytes (Makita et al., 1994). Although there is evidence that β_1 exists in heart tissues in vivo (Nuss et al., 1995; Makielski et al., 1996; also see review by Fozzard and Hanck, 1996), its effect on either gating or slow inactivation of hH1 channels is, as yet, unknown.

Slow inactivation and ultraslow inactivation in hSkM1 and hH1 Na^+ channels can be modulated by mutating elements of their conductance pore (S5-S6 linkers, or P-loops) (Cummins and Sigworth, 1996; Makita et al., 1996; Hayward et al., 1997; Todt et al., 1999). These data point toward the structural determinants of slow inactivation. In this study we describe alterations of slow inactivation in

hSkM1 and hH1 sodium channels, induced by changes in the molecular structure of hSkM1 P-loop, and by coexpression of the β_1-subunit with hSkM1, hH1, and chimeric (hSkM1-hH1/P1234) sodium channel α-subunits. Briefly, transposing all four hH1 P-loops into a hSkM1 backbone confers hH1-like slow inactivation properties on the chimeric construct. Furthermore, the β_1-subunit modulates completion of slow inactivation in hSkM1 but not hH1 sodium channels.

MATERIALS AND METHODS

hSkM1 and hH1 sodium channels were constructed as previously described (Featherstone et al., 1996; Richmond et al., 1998). The pore-loop hSkM1/hH1 chimera was constructed as described (Makita et al., 1996). The hSkM1-P1234 chimera (D1234P), in which all four P-loops were substituted with the corresponding sequences from hH1, was assembled by directional ligation of restriction fragments from hSkM1-P12 and hSkM1-P34. The final construct was sequenced to verify the presence of all four transplanted hH1 sequences. The hSkM1-P1234 chimera contains the following amino acid substitutions: amino acids 278–422 of hSkM1 replaced by hH1 residues 278–388; hSkM1 residues 725–784 replaced by hH1 804–921; hSkM1 1187–1273 replaced by hH1 1361–1448; and hSkM11512–1573 replaced by hH1 1678–1747. The β_1-subunit was a gift from L. Isom (Isom et al., 1992). Equal volumes of α-subunit (concentration of ~1 μg/μl) of each clone and β_1-subunit mRNA (concentration of ~2 μg/μl) were mixed together and then injected.

Stage V-VI oocytes were surgically removed from female *Xenopus laevis* (Nasco, Modesto, CA) anesthetized with 0.17% tricaine methanesulfonate (Sigma, St. Louis, MO). After surgery, frogs recovered in isolation in a shallow tank of distilled water. After full recovery, frogs were returned to the large rearing tank. Frogs routinely undergo up to six surgeries (at a frequency of less than one surgery every 2 months) with no obvious ill effects. After six surgeries, frogs are anesthetized and sacrificed by freezing under anesthesia, in accordance with institutional guidelines.

Theca and follicle cells were enzymatically removed by gently agitating the oocytes in a solution containing (in mM) 96 NaCl, 2 KCl, 20 $MgCl_2$, 5 HEPES (pH 7.4), with 2 mg/ml collagenase (Sigma) for ~1 h. After enzymatic treatment, oocytes were rinsed several times in a solution containing (in mM) 96 NaCl, 2 KCl, 20 $MgCl_2$, 5 HEPES (pH 7.4), then placed in sterile incubation medium containing (in mM) 96 NaCl, 2 KCl, 20 $MgCl_2$, 1.8 $CaCl_2$, 5 HEPES, 2.5 pyruvic acid (pH 7.4), with 1–5% horse serum (Hyclone Laboratories, Logan, UT) and 1 mM gentamicin sulfate (100 mg/liter) at 18°C. Approximately 24 h after enzymatic treatment, oocytes were individually injected with 50 nl of mRNA, using a Drummond automatic injector, and then further incubated in disposable 60-mm Petri dishes with gentle agitation (~60 rpm on a small rotary shaker) at 18°C until electrophysiological recording 3–14 days later. The incubation solution bathing the oocytes was changed daily. In the experiment where we tested the effect of the β_1-subunit on steady-state slow inactivation, α- and β_1-subunits were coinjected as a 1:1 volume mixture (Richmond et al., 1998).

Before macropatch recording, the vitelline membrane was manually removed from oocytes after a short (2–5 min) exposure to a hyperosmotic solution containing (in mM) 96 NaCl, 2 KCl, 20 $MgCl_2$, 5 HEPES, 400 mannitol (pH 7.4). All macropatch recording was done in a chamber containing (in mM) 9.6 NaCl, 88 KCl, 11 EGTA, 5 HEPES (pH 7.4). Aluminosilicate patch electrodes were pulled on a Sutter P-87, dipped in melted dental wax to reduce capacitance, fire polished, and filled with (in mM) 96 NaCl, 4 KCl, 1 $MgCl_2$, 1.8 $CaCl_2$, 5 HEPES (pH 7.4).

Electrophysiological recordings were made using an EPC-9 patch-clamp amplifier (HEKA Elektronik Gmbh, Lambrecht, Germany) and digitized at 5 kHz (bandwidth before digitization was 1 MHz) via an ITC-16 interface (Instrutech, Great Neck, NY). Voltage clamping and data acquisition were controlled via Pulse software (HEKA Elektronik Gmbh) running on a G3 Power Macintosh. All data were software-low-pass-filtered at 5 kHz during acquisition. The experimental bath temperature was maintained at 22 ± 0.2°C for all experiments by using a Peltier device controlled by an HCC-100A temperature controller (Dagan, Minneapolis, MN). After seal formation, patches were left on-cell for all recordings.

Sodium channel slow inactivation can be experimentally separated from fast inactivation by using enzymatic removal of fast inactivation, mutating the IFM motif in the III-IV linker, or with pulse protocols designed to allow fast inactivation to recover before assessing the number of slow inactivated channels. However, enzymatic treatments can produce collateral effects on processes other than fast inactivation, and mutating the IFM motif has impacts on slow inactivation as well as removing fast inactivation. We thus chose the kinetic method to study the onset, recovery, and completion of slow inactivation in skeletal muscle and cardiac sodium channels, and a skeletal/cardiac chimera, in both the presence and the absence of the β_1-subunit.

Because the study of slow inactivation required long recording durations and extended bouts of pulsing, we were very careful to avoid time- and pulsing-related artifacts, which add anomalous time constants to inactivation and recovery. When the voltage dependence of inactivation was studied, Pulse clamp control software (HEKA Elektronik Gmbh) alternated prepulse potentials, such that prepulse potentials were delivered as −160 mV, +10 mV, −155 mV, +5 mV, −150 mV, etc. over the voltage range of −160 mV to +10 mV in 5-mV steps. Time-related distortions of steady-state slow inactivation curves were further avoided by gathering data by two prepulse protocols: first the voltage was stepped to all "even" voltages (e.g., −160, 0, −140, −20 mV, etc.), followed next by "odd" voltages (e.g., −150, −10, −130, −30 mV, etc.). Before every slow inactivation prepulse, we always allowed 30 s at −180 mV to ensure complete recovery from all inactivation and avoid any accumulation of inactivation throughout the experiment. The prepulse duration for steady-state slow inactivation was 1 min.

The holding potential for all experiments was −150 mV. Leak subtraction was performed automatically by the software, using a p/4 protocol. Leak pulses alternated in direction from a holding potential of −120 mV. Leak pulses were always performed after the test pulse, and sufficient time between protocols was allowed to ensure that the leak pulses would have no effect on the data. Subsequent analysis and graphing were done using Pulsefit (HEKA Elektronik Gmbh) and Igor Pro (Wavemetrics, Lake Oswego, OR), both run on a G3 Power Macintosh.

Kinetics of recovery and onset of slow inactivation were obtained as previously described (Featherstone et al., 1996; Richmond et al., 1998). Time constants (τ) for onset (and recovery) of slow inactivation were derived from monoexponential fitting to peak current amplitude versus prepulse (or interpulse) duration:

$$I = I_{SS} + a_1 \exp(-t/\tau)$$

where I is current amplitude, I_{SS} is the steady-state current or asymptote (plateau amplitude), a_1 is the amplitude at time = 0 (time of peak current), and τ is the time constant (in ms). Completion of steady-state slow inactivation was derived from the lowest plateau of steady-state inactivation curves.

Pulse protocols

The steady-state slow inactivation pulse protocol was as described above.

The onset of slow inactivation was measured as follows: 1) sodium channels were held at −150 mV for 30 s to eliminate both fast and slow inactivation; 2) a prepulse of 0–60 s (variable increments) at −90 mV, −30 mV, and 0 mV was applied to induce slow inactivation; 3) a 20-ms pulse to −150 mV selectively recovered fast inactivated channels before the test pulse; 4) the amplitudes of sodium currents elicited in response to a 0-mV test pulse were plotted as normalized current amplitude versus prepulse duration, for each interpulse voltage, and used to measure the onset of slow inactivation; 5) an additional 30-s pulse at −150 mV was used to avoid any possible accumulation of slow inactivation.

Recovery from slow inactivation was studied as follows: 1) channels were slow inactivated by applying a 60-s prepulse to 0 mV; 2) 0–60-s interpulse durations (variable increments) at −110 mV, −130 mV, and −150 mV were used to recover channels from slow inactivation; 3) a 20-ms pulse to −150 mV was used to selectively recover fast inactivated channels before the test pulse; 4) the peak current amplitudes that were elicited by a 0-mV test pulse were plotted as normalized current amplitude versus interpulse duration for each recovery voltage.

All statistical values, both in the text and in the figures, are given as mean ± standard error (SEM). Exponential fits were performed for each data set to obtain mean ± standard error values for the time constants. Statistical differences were derived from Student's *t*-tests, using a statistical software package (Instat; GraphPad Software, San Diego, CA).

RESULTS

Coexpression of the β_1-subunit modulates steady-state slow inactivation in hSkM1 but not in hH1 sodium channels

In this series of experiments we examined steady-state slow inactivation in hSkM1 skeletal muscle and hH1 cardiac sodium channels in the absence of the β_1-subunit (hSkM1 − β_1 and hH1 − β_1) and when β_1 was coexpressed (hSkM1 + β_1 and hH1 + β_1). Fig. 1, *A* and *B*, shows traces of typical sodium currents with and without β_1 obtained with the pulse protocol shown in the Fig. 1 inset. In Fig. 1 *C*, steady-state slow inactivation in hSkM1 + β_1 (*filled circles*) and hSkM1 − β_1 (*filled squares*) is plotted as normalized current amplitude versus 60-s prepulse voltage. The smallest sodium current amplitudes from hSkM1 + β_1 (Fig. 1 *A*) and hSkM1 − β_1 (Fig. 1 *B*) correspond to the most complete slow inactivation of hSkM1 + β_1 (Fig. 1 *C, filled circles*) and steady-state slow inactivation of hSkM1 − β_1 (Fig. 1 *C, filled squares*), respectively. In hSkM1 + β_1, slow inactivation completion reaches 85.5% (± 2.9, $N = 7$). These data are consistent with previously published results (Featherstone et al., 1996). Steady-state slow inactivation in hSkM1 − β_1 is complete at 56.7% (± 2.5, $N = 8$). Thus steady-state slow inactivation in hSkM1 + β_1 sodium channels is dramatically different from steady-state slow inactivation in hSkM1 − β_1 channels. We verified these results using an alternative method of assessing steady-state slow inactivation. Fig. 1 *C* includes asymptotes derived from monoexponential fits to slow inactivation onset and slow inactivation recovery data, such as those shown in Fig. 2, *A–D*. These asymptotes agree well with the 60-s prepulse slow inactivation data for both hSkM1 + β_1 and the hSkM1 − β_1 sodium channels, suggesting that steady-state slow inactivation was complete, and no slower components of slow inactivation were missed.

Fig. 1, *D* and *E*, shows typical sodium currents from human cardiac sodium channels expressed without β_1-subunit (hH1 − β_1) and hH1 channels coexpressed with β_1-subunit (hH1 + β_1), respectively. These currents were obtained with the same pulse protocol (Fig. 1, *inset*) used to measure steady-state slow inactivation. As shown in Fig. 1 *F*, steady-state slow inactivation in hH1 − β_1 sodium channels reached completion at 46% (± 3.4, $N = 7$; *filled circles*). These data agree well with previously published data (Richmond et al., 1998). In hH1 + β_1 (Fig. 1 *F, filled squares*), steady-state slow inactivation reaches completion at 45% (± 3.5, $N = 7$; *filled squares*), very close to that seen in hH1 − β_1. Asymptotes shown in Fig. 1 F are derived from monoexponential fits to the onset of, and recovery from, slow inactivation shown in Fig. 3, *A–D*. These asymptotes closely correspond to steady-state slow inactivation data for both hH1 − β_1 and the hH1 + β_1 sodium channels measured using 60-s prepulses. Thus Fig. 1 *F* demonstrates that there is no discernible effect of β_1 coexpression on steady-state slow inactivation in hH1 sodium channels.

The β_1-subunit alters the rates of slow inactivation in hSkM1 and hH1 sodium channels

Figs. 2 *A* and 2 *C* show, respectively, the recovery from slow inactivation and onset of slow inactivation for hSkM1 + β_1 channels. The kinetics of slow inactivation recovery and onset in hSkM1 − β_1 sodium channels are shown in Figs. 2 *B* and 2 *D*, respectively. In Fig. 2 *E*, the voltage dependence of the slow inactivation time constants for hSkM1 + β_1 and hSkM1 − β_1 channels is shown. Generally, slow inactivation time constants for hSkM1 + β_1 and hSkM1 − β_1 sodium channels are not very different (Fig. 2 *E*). Only time constants for the most positive voltages (−30 mV, $p = 0.0143$; 0 mV, $p = 0.0037$) differ between hSkM1 − β_1 and the hSkM1 + β_1 sodium channels. A comparison of onset kinetics between Fig. 2 *C* and Fig. 2 *D* shows that slow inactivation in hSkM1 + β_1 channels (Fig. 2 *C*) is more complete than in the hSkM1 − β_1 channels (Fig. 2 *D*; see also Fig. 1 *C*). The kinetics of recovery in hSkM1 + β_1 and hSkM1 − β_1 sodium channels are very similar (Fig. 2, *A* and *B*).

The kinetics of slow inactivation in hH1 channels in the presence and absence of the β_1-subunit were also examined, using the same set of pulse protocols as described for experiments with hSkM1 skeletal sodium channels. Fig. 3 *A* and Fig. 3 *B* show, respectively, the recovery from slow inactivation in hH1 + β_1 and hH1 − β_1. Two voltages for the 0–60-s interpulse are shown: −130 mV (*filled circles*, hH1 + β_1; *open circles*, hH1 − β_1) and −150 mV (*filled squares*, hH1 + β_1; *open squares*, hH1 − β_1). Fig. 3 *C* shows the results from onset experiments in hH1 + β_1 channels. Three voltages for hH1 + β_1 are shown: −30 mV (*filled circles*), −50 mV (*filled squares*), and −70 mV (*filled triangles*). Three voltages for hH1 − β_1 are shown in Fig. 3 *D*: 0 mV (*open circles*), −30 mV (*open squares*), and −50 mV (*open triangles*). Data were fitted with a single exponential, and time constants of slow inactivation were obtained as described above. Slow inactivation time constants in hH1 + β_1 (*filled circles*) and hH1 − β_1 (*open circles*) are plotted against the prepulse voltage in Fig. 3 *E*. Because our experiments in hH1 − β_1 did not reveal clear kinetics of slow inactivation onset at −110 mV, −90 mV,

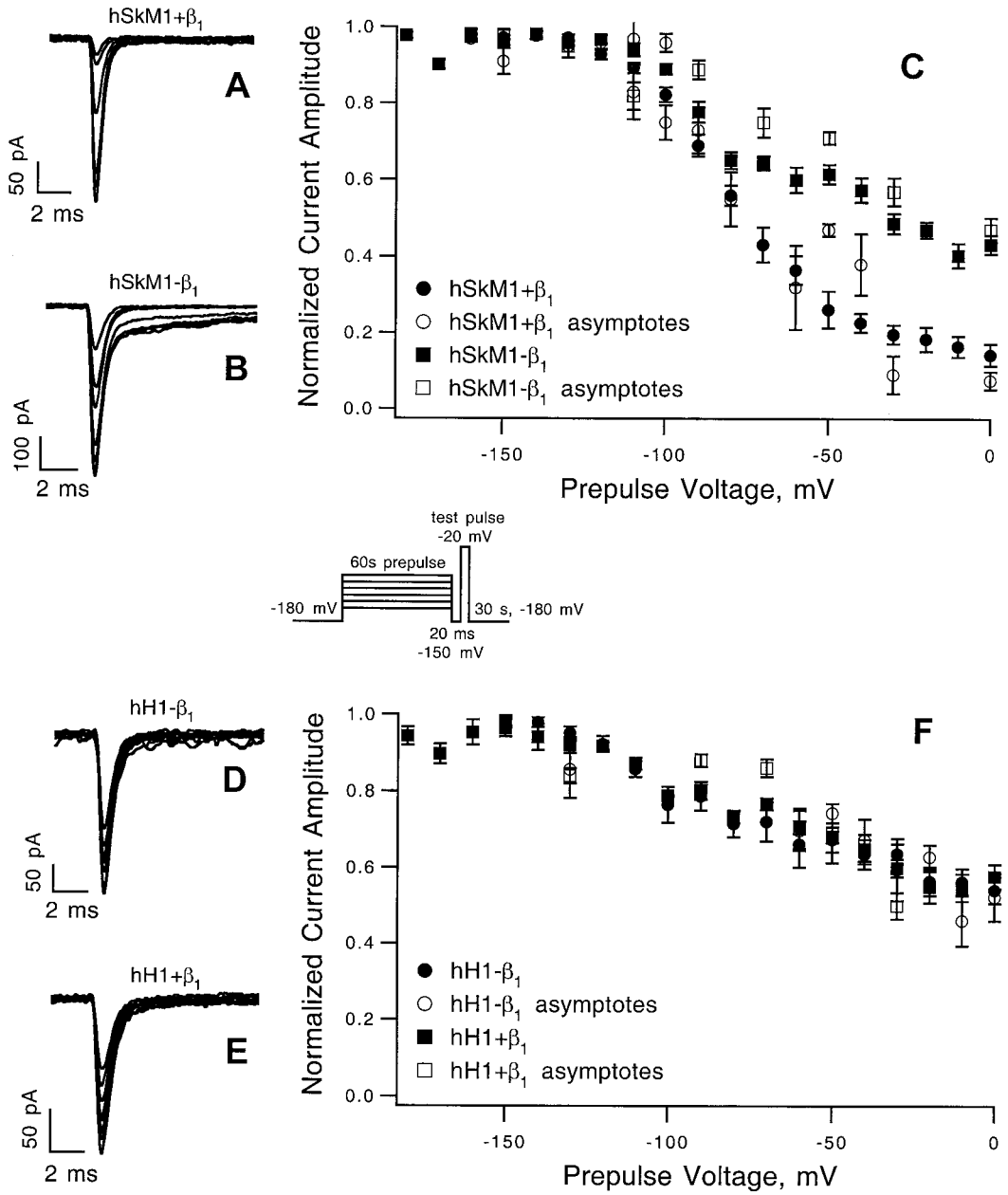

FIGURE 1 Effect of β_1-subunit coexpression on steady-state slow inactivation in hSkM1 skeletal and hH1 cardiac sodium channels. (*A* and *B*) Typical current records for hSkM1 + β_1 and hSkM1 − β_1 sodium currents obtained after a 60-s prepulse, respectively. Prepulse was changed from −180 mV to 0 mV. (*C*) The steady-state slow inactivation of hSkM1 + β_1 (●, $N = 7$) and hSkM1 − β_1 (■, $N = 8$) sodium channels is plotted as average normalized current amplitude versus 60-s prepulse voltage. Asymptotes for hSkM1 + β_1 (○, N ranges from 3 to 7) and hSkM1 − β_1 (□, N ranges from 5 to 9) are shown in *C* from exponential fits to the onset and recovery of slow inactivation curves at each voltage tested (summarized in Fig. 2, *A–D*). (*D* and *E*) Typical traces for hH1 − β_1 and hH1 + β_1 sodium currents, obtained using the same pulse protocol as above. (*F*) The steady-state slow inactivation of hH1 + β_1 (■, $N = 5$) and hH1 − β_1 (●, $N = 7$) sodium channels and asymptotes for hH1 + β_1 (□, N ranges from 4 to 7) and hH1 − β_1 (○, N ranges from 3 to 7) are shown.

or −70 mV, these points were not calculated or included in the present figure (Richmond et al., 1998). hH1 + β_1 also have highly variable kinetics of recovery from slow inactivation at −110 mV. This point is also not shown. Coexpression of hH1 with β_1 accelerates time constants in the middle voltage range (Fig. 3 *E, filled circles*). This finding may indicate that β_1 has some interaction with the α-subunit of hH1 cardiac sodium channels.

Substitution of S5-S6 P-loops in hSkM1 skeletal sodium channels by the S5-S6 P-loops from hH1 cardiac sodium channels alters steady-state slow inactivation and the time constants of slow inactivation

In the previous series of experiments, we found that the absence of β_1-subunit in hSkM1 channels lowers the com-

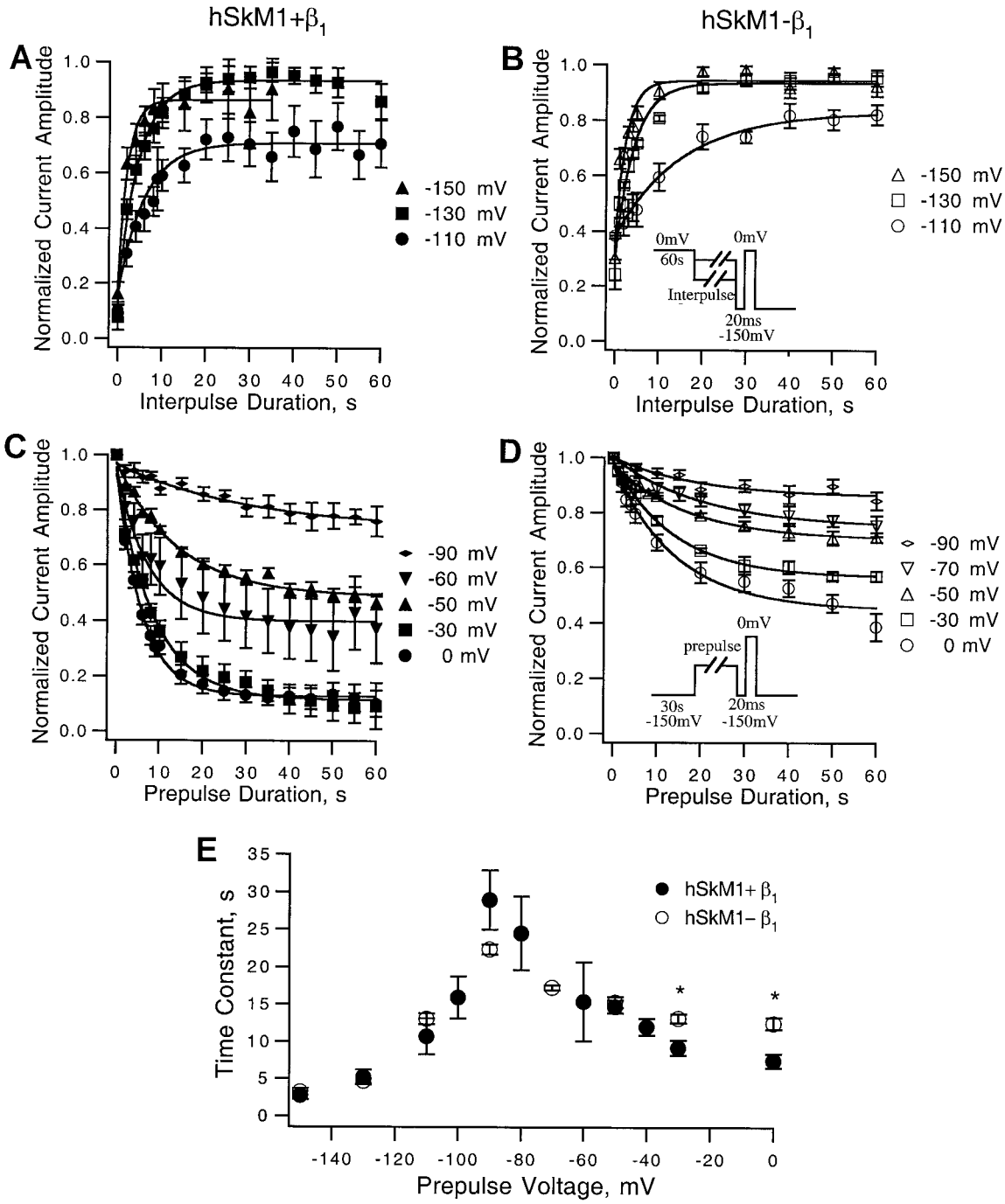

FIGURE 2 Effect of β_1-subunit on the kinetics of slow inactivation in hSkM1 skeletal sodium channels. (*A* and *B*) The time course of recovery from slow inactivation for hSkM1 + β_1 (*N* ranges from 4 to 10) and hSkM1 − β_1 (*N* ranges from 7 to 9), respectively. The averaged, normalized currents obtained at the 0-mV test pulse after an interpulse period of increasing duration over a range of potentials (−150 mV to −110 mV) are plotted against the duration of the interpulse period and fit with a single exponential. (*C* and *D*) The time course of slow inactivation onset for hSkM1 + β_1 (*N* ranges from 3 to 8) and hSkM1 − β_1 (*N* ranges from 5 to 7) skeletal sodium channels. Currents were obtained at 0-mV test pulse after a prepulse period of increasing duration over a range of voltages (−90 mV to 0 mV). Averaged, normalized currents are plotted against the duration of the prepulse period and fit with a single exponential. (*E*) The averaged time constants for slow inactivation in hSkM1 + β_1 (●) and hSkM1 − β_1 (○) derived from single-exponential fits to all of the data shown in *A–D*. Time constants are plotted versus the prepulse voltage. All values represent mean ± SEM (significant differences are denoted by *).

pletion of slow inactivation to ~57% (see Figs. 1 *A*, 1 *B*, 1 *C*, and 2 for details). By contrast, coexpression of β_1 with hH1 channels did not have a significant effect on steady-state slow inactivation (slow inactivation is completed at ~45% in both hH1 + β_1 and hH1 − β_1 channels; Figs. 1 *D*, 1 *E*, and 1 *F*). Because the absence of β_1 did not reduce the completion level of steady-state slow inactivation in hSkM1 channels to that of hH1, we surmised that there must be

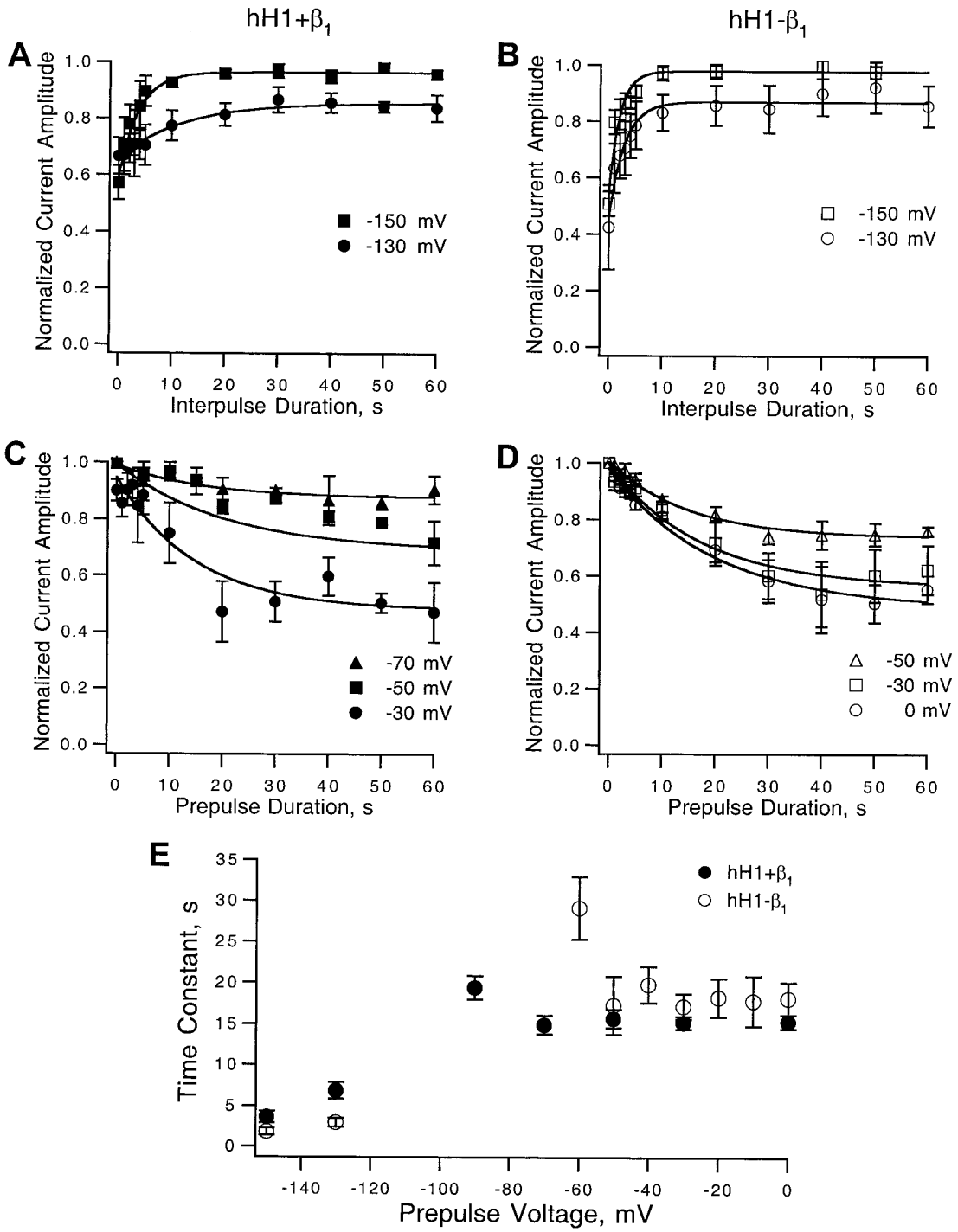

FIGURE 3 Effect of the β_1-subunit on the kinetics of slow inactivation in hH1 cardiac sodium channels. (*A* and *B*) The time course of recovery from slow inactivation for hH1 + β_1 (*N* ranges from 7 to 9) and hH1 − β_1 (*N* ranges from 4 to 10), respectively. The averaged, normalized currents obtained at the 0-mV test potential after a interpulse period of increasing duration over a range of recovery voltages (two voltages are shown: −150 mV and −130 mV; see text) are plotted against interpulse duration and fit with a single exponential. (*C* and *D*) The time course of slow inactivation onset for hH1 + β_1 (*N* ranges from 5 to 7) and hH1 − β_1 (*N* ranges from 3 to 8), respectively. Average, normalized currents obtained at 0 mV are plotted against prepulse duration and fit with a single exponential. (*E*) The averaged time constants for slow inactivation in hH1 + β_1 (●) and hH1 − β_1 (○) derived from single-exponential fits to all of the data shown in *A–D*. All values represent mean ± SEM.

another reason for the difference in steady-state slow inactivation between the two channel isoforms.

Several lines of research have suggested that slow inactivation gating may involve the conductance pathway. We therefore sought to elucidate the role of the P-loop (S5-S6 P-loops) in slow inactivation of hSkM1 and hH1 sodium channels. An hSkM1/hH1 chimera (D1234P) was used, wherein each P-loop in hSkM1 was replaced with the cor-

responding P-loop from hH1 sodium channels. The remainder of hSkM1 α-subunit was left as wild type. The D1234P chimera was coexpressed with and without the β_1-subunit (D1234P + β_1 and D1234P − β_1). Fig. 4, *A* and *B*, shows typical sodium current records from D1234P + β_1 and D1234P − β_1, obtained with the pulse protocol shown in Fig. 4 *C* (*inset*). It is apparent that the coexpression of the β_1-subunit does not change the kinetics of these traces. In Fig. 4 *C*, steady-state slow inactivation for both D1234P + β_1 (*filled circles*) and D1234P − β_1 (*filled squares*) is plotted as normalized current amplitudes versus a 60-s prepulse voltage. Slow inactivation is complete at similar levels: 45.5% (± 2.7, $N = 7$) for D1234P + β_1, and 47% (± 2.4, $N = 5$) for D1234P − β_1. Interestingly, the completion of slow inactivation for D1234P + β_1 and D1234P − β_1 is similar to that for hH1 cardiac sodium channels (~45% for hH1 channels; see Fig. 3 *E*). The data in Fig. 4 *C* are also confirmed by asymptotes from monoexponential fits to slow inactivation onset and recovery data (data not shown). Pulse protocols used to measure recovery and onset of slow inactivation are shown in the inset in Fig. 4 *D*. Fig. 4 *D* demonstrates the voltage dependence of slow

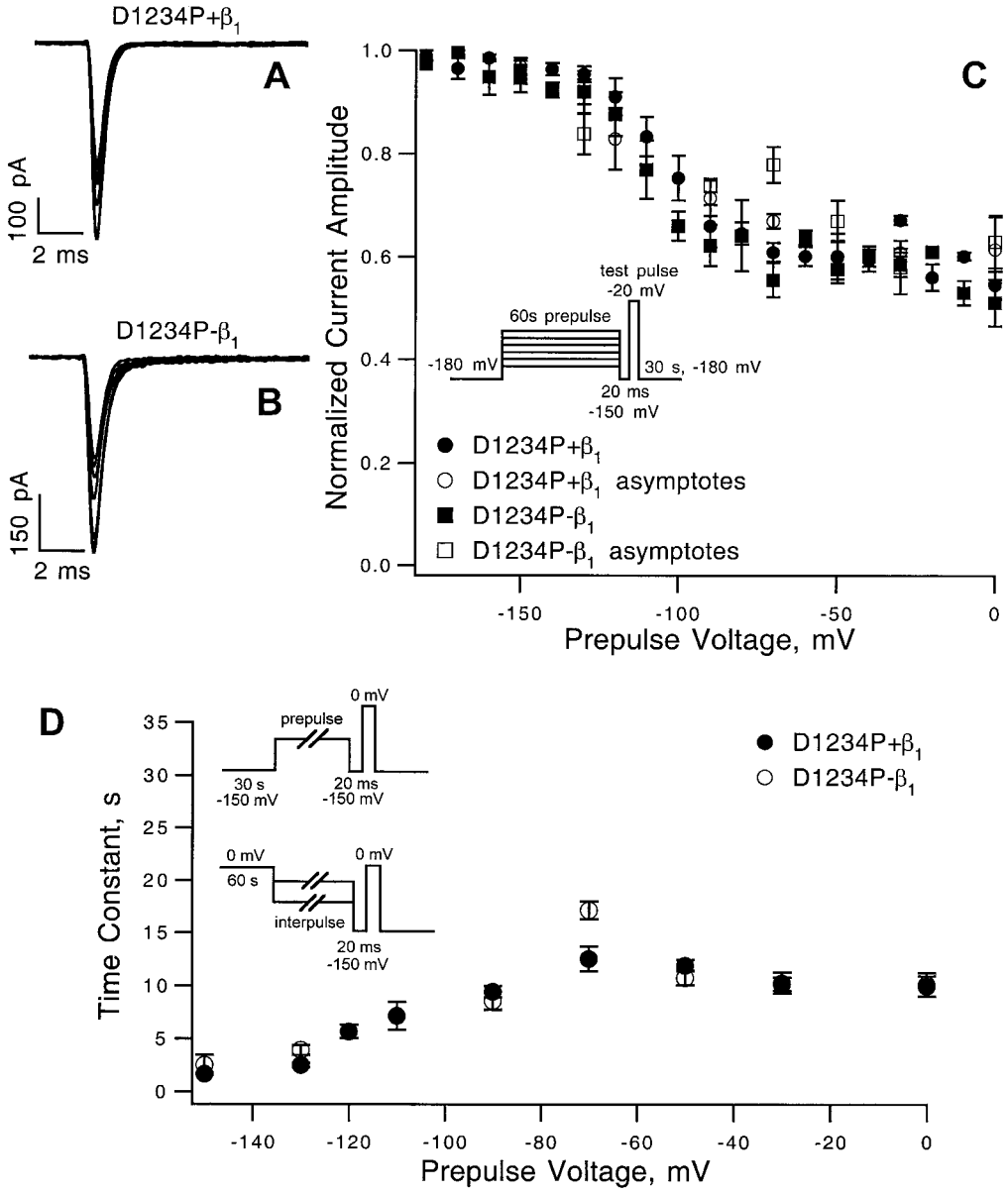

FIGURE 4 Slow inactivation in the chimera D1234P. (*A* and *B*) Typical current records from D1234P + β_1 and D1234P − β_1, respectively. The pulse protocol was the same as in Fig. 1. (*C*) Steady-state slow inactivation of D1234P + β_1 (●, $N = 7$) and D1234P − β_1 (■, $N = 5$) sodium channels is plotted as average normalized current amplitude versus 60-s prepulse voltage. Asymptotes for D1234P + β_1 (○, N ranges from 4 to 9) and D1234P − β_1 (□, N ranges from 3 to 7) were added to *C* from exponential fits to the time courses of onset and recovery of slow inactivation (data are not shown). (*D*) The averaged time constants for slow inactivation in D1234P + β_1 (●) and D1234P − β_1 (○) derived from single-exponential fits to the onset and recovery of slow inactivation. Time constants are plotted versus prepulse voltage. All values represent mean ± SEM.

inactivation time constants for D1234P + β_1 (*filled circles, N* = 3–8) and D1234P − β_1 (*open circles, N* = 4–7) sodium channels. Coexpression of the β_1-subunit has little effect on the time constants of D1234P slow inactivation, but replacing hSkM1 P-loops with hH1 P-loops significantly accelerates the time constants compared to those of hH1 and hSkM1 sodium channels ($p < 0.05$; see also Figs. 2 *E* and 3 *E*). Thus these data support the idea that the P-region might be a structural determinant of slow inactivation in sodium channels.

A comparison of β_1-subunit and P-loop modulation of slow inactivation in hSkM1 and hH1 sodium channels

Fig. 5 is a summary of changes in steady-state slow inactivation seen in this study. The levels of completion for slow inactivation are presented as histograms. Comparing the effects of the β_1-subunit reveals some interesting results. Slow inactivation in hSkM1 muscle sodium channels, but not hH1 sodium channels, is dramatically affected by the β_1-subunit. hSkM1 + β_1 reaches the most complete level of slow inactivation (86.5 ± 2.95%, $N = 7$). When these channels are expressed without the β_1-subunit, slow inactivation is significantly reduced to 56.7% completion (±2.5, $N = 8$; $p < 0.0001$). In contrast, the difference in completion between hH1 + β_1 and hH1 − β_1 is not significant ($p = 0.87$). Slow inactivation in hSkM1 − β_1 channels is never as incomplete as either hH1 + β_1 or hH1 − β_1 channels ($p = 0.023$). This difference can be explained by the results of experiments using the D1234P chimera. Comparing hH1 + β_1 and hH1 − β_1 on the one hand and D1234P + β_1 and D1234P − β_1 on the other shows the remarkable similarity in the completion of slow inactivation for the four channel types. The β_1 does not affect completion of slow inactivation in D1234P or hH1 channels ($p = 0.8$). D1234P channels have the least complete slow inactivation: 46% for D1234P + β_1 (± 2.7, $N = 7$) and 45.5% for D1234P − β_1 (± 2.4, $N = 5$).

DISCUSSION

The goal of this study was to explore the structural determinants of slow inactivation in skeletal and cardiac sodium channels, and to account for the differences between these two isoforms. The fundamental structure/function relationships in hSkM1 and hH1 sodium channels are an important tool in clarifying mechanisms of slow inactivation. Mechanisms of sodium channel fast inactivation, as well as studies of C-type inactivation in K^+ channels, have provided insights into the structural substrates of slow inactivation in sodium channels (Hoshi et al., 1990; 1991; Isacoff et. al., 1991). It is clear that the structural determinants of fast inactivation are distinct from those of slow inactivation, because replacement of the IFM motif removes only fast inactivation (West et al., 1992; Featherstone et al., 1996). Ionic strength affects C-type inactivation in potassium channels (Levy and Deutsch, 1996), as well as slow inactivation in sodium channels (Townsend and Horn, 1997). These studies suggest where the structural determinants for slow inactivation might (the P-region) and might not (the III-IV linker) be found.

The importance of the β_1-subunit in modulating fast inactivation in hSkM1 sodium channels has been demonstrated (Isom et al., 1994; Chen and Cannon, 1995). Here we describe a significant role of the β_1-subunit in the modulation of slow inactivation in hSkM1 channels (Fig. 1, *A–C*). Coexpression of the β_1-subunit increases the completion of slow inactivation from ~57% to ~85% in hSkM1 channels (Fig. 1 *C*). In contrast, β_1 does not affect slow inactivation in hH1 sodium channels (Fig. 1, *D–F*). Interestingly, the β_1-subunit also has little or no effect on fast inactivation in hH1 channels (see review in Fozzard and Hank, 1996). β_1 does not affect the time constants of slow inactivation in hSkM1 sodium channels (Fig. 2), but accelerates slow inactivation onset and recovery in hH1 sodium channels (Fig. 3). These data suggest that β_1 has different specific mechanisms of interaction with the α-subunits of hSkM1 and hH1 sodium channels.

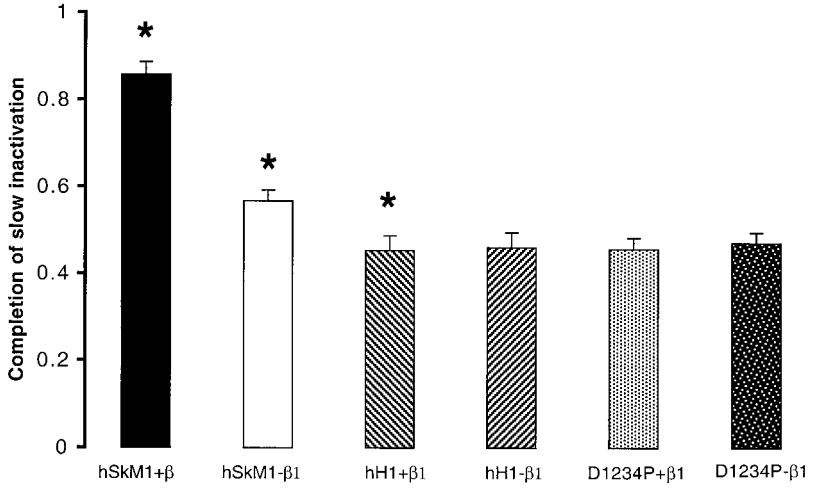

FIGURE 5 Comparison of effects on steady-state slow inactivation of β_1-subunit coexpression and replacement of S5-S6 P-loops in hSkM1 channels with S5-S6 P-loops from hH1 channels. Completion levels of slow inactivation are derived from data in Figs. 1 *C*, 1 *F*, and 4 *C* as described in Materials and Methods. Asterisks denote statistically significant differences in completeness of slow inactivation between hSkM1 + β_1 with hSkM1 − β_1 ($p < 0.0001$), and hSkM1 + β_1 with hH1 + β_1 sodium channels ($p < 0.0001$).

Recently published data indicate that the pore region (P-loops) in hH1 and hSkM1 could be determinants of β_1-induced gating modulation in sodium channels (Makita et al., 1996). In our experiments, using a chimera in which all of the P-loops in hSkM1 channels were replaced with the P-loops from hH1, completion of slow inactivation in these channels is dramatically changed (Fig. 4 *C*). It is important to emphasize that slow inactivation in hH1 channels is as complete as in D1234P sodium channels (Figs. 1 *F* and 4 *C*). Therefore, replacing hSkM1 P-loops with hH1 P-loops produces hH1-like completion of slow inactivation in hSkM1 channels. The inability of β_1 to alter the completion of steady-state slow inactivation in hH1 (Fig. 1 *F*) is also found in D1234P + β_1 and D1234P − β_1 (see Fig. 4 *C*). On the other hand, β_1 slightly accelerates slow inactivation time constants for D1234P, in contrast to the much stronger acceleration of time constants for both D1234P + β_1 and D1234P − β_1 channels (relative to hSkM1) due to P-loop replacement (see Fig. 4 *D*). Thus data shown in Fig. 4 indicate that profound changes in both completion of slow inactivation and slow inactivation time constants for D1234P sodium channels are caused by specific structural features of the hH1 P-loop and are less affected by the coexpression of the β_1-subunit. To compare the effects of β_1 coexpression and P-loop substitution on slow inactivation, the levels of completion of steady-state slow inactivation for every studied case (hSkM1 + β_1, hSkM1 − β_1, hH1 + β_1, hH1 − β_1, D1234P + β_1, and D1234P − β_1) are presented as histograms in Fig. 5. According to our data, P-loop substitution has a strong impact on the completion of steady-state slow inactivation. β_1 strongly modulates slow inactivation in hSkM1, but not in hH1 or D1234P sodium channels. This raises an interesting question about the functional role of β_1 modulation of hH1 channels. Despite the evidence that β_1-subunits coexist in vivo with hH1 α-subunits, the role of β_1 in this molecular complex is still questionable (Makita et. al., 1994). The precise structural basis of possible α-β_1 interactions in hH1 is as yet unknown, and the interactions between α- and β_1-subunits in hSkM1 channels are not completely characterized (McCormick et al., 1998).

These data allow us to suggest that the gates of slow inactivation in sodium channels may be localized within the S5-S6 loops. This hypothesis could explain the differences in slow inactivation between hSkM1 − β_1 and hH1 − β_1 (see Fig. 5). This idea is consistent with previously published data (Makita et al., 1996; Wang and Wang, 1997), as well as information on the structural substrates of C-type inactivation in K^+ channels (Liss et al., 1999). It is interesting that the P-loop has the role of conductance pore (Catterall, 1993; Fozzard and Hanck, 1996; Balser et al., 1996; Marban et al., 1998) and is also apparently involved in inactivation gating. A collapse of the ionic conduction pathway would be a convenient means of inducing slow inactivation (Townsend and Horn, 1997; see also Ruff, 1996). This mechanism would be consistent with previous findings concerning 1) the apparent voltage dependence of slow inactivation (Ruben et al., 1992), whereby movements of putative S4 voltage sensors might induce changes in the pore conformation (as in activation), and 2) limitation of slow inactivation by the DIII-DIV IFM putative fast inactivation particle (Featherstone et al., 1996; but see Vedantham and Cannon, 1998). In addition, changes in the extracellular ionic environment affect both the kinetics and steady-state level of slow inactivation in hH1 sodium channels (Townsend and Horn, 1997). Previously published data also indicate that the β_1-subunit possibly interacts with one or more S5-S6 P-loops (Makita et al., 1996; McCormick et al., 1998). Results presented here support this idea. Future studies with single or multiple P-loop substitution will provide more detailed information on the structural underpinnings of slow inactivation in sodium channels.

The authors thank Jennifer Abbruzzese and Shana Geffeney for critically reading the manuscript and Esther Fujimoto for RNA preparation.

This project was supported by funds from the Muscular Dystrophy Association, a Public Health Service (PHS) grant R01-NS29204 to PCR, and a PHS grant NS32387 to ALG.

REFERENCES

Armstrong, C. M., and F. Bezanilla. 1977. Inactivation of the sodium channel. II. Gating current experiments. *J. Gen. Physiol.* 70:567–590.

Balser, J. R., H. B. Nuss, N. Chiamvimonvat, M. T. Perez-Garcia, E. Marban, and G. Tomaselli, 1996. External pore residue mediates slow inactivation in μ_1 rat skeletal muscle sodium channels. *J. Physiol. (Lond.).* 494.2:431–442.

Cannon, S. C., A. I. McClatchey, and J. F. Gusella. 1993. Modification of Na^+ current conducted by the rat skeletal muscle α subunit by coexpression with a human brain β subunit. *Pflügers Arch.* 423:155–157.

Catterall, W. A. 1993. Structure and function of voltage-gated ion channels. *Trends Neurosci.* 16:500–506.

Chandler, W. K., and H. Meves. 1970. Slow changes in membrane permeability and long-lasting action potentials in axons perfused with sodium fluoride. *J. Physiol. (Lond.).* 211:707–728

Chen, C., and S. C. Cannon. 1995. Modulation of Na^+ channel inactivation by the β_1 subunit: a deletion analysis. *Pflügers Arch.* 431:186–195.

Cummins, T. R., and F. J. Sigworth. 1996. Impaired slow inactivation in mutant sodium channels. *Biophys. J.* 71:227–236.

Featherstone, D. E., J. E. Richmond, and P. C. Ruben. 1996. Interaction between fast and slow inactivation in Skm1 sodium channels. *Biophys. J.* 71:3098–3109.

Fleidervish, I. A., A. Freidman, and M. J. Gutnick. 1996. Slow inactivation of Na^+ current and slow cumulative spike adaptation in mouse and guinea-pig neocortical neurones in slices. *J. Physiol. (Lond.).* 493.1: 83–97.

Fozzard, H. A., and D. A. Hanck. 1996. Structure and function of voltage-dependent sodium channels: comparison of brain II and cardiac isoforms. *Physiol. Rev.* 76:887–926.

Gellens, M. E., A. L. George, J. Chen, L. Q. Chahine, M. Horn, R. L. Barchi, and R. G. Kallen. 1992. Primary structure and functional expression of the human cardiac tetrodotoxin-insensitive voltage-dependent sodium channels. *Proc. Natl. Acad. Sci. USA.* 89:554–558.

George, A. L., J. Komisarof, R. G. Kallen, and R. L. Barchi. 1992. Primary structure of the adult human skeletal muscle voltage-dependent sodium channels. *Ann. Neurol.* 31:131–137.

Hayward, L. J., R. H. Brown, and S. C. Cannon. 1997. Slow inactivation differs among mutant Na channels associated with myotonia and periodic paralysis. *Biophys. J.* 72:1204–1219.

Hayward, L. J., G. M. Sandoval, and S. C. Cannon. 1999. Defective slow inactivation of sodium channels contributes to familial periodic paralysis. *Neurology.* 52:1447–1453.

Hille, B. 1992. Ionic Channels of Excitable Membranes. Sinauer Associates, Sunderland, MA.

Hodgkin, A. L., and A. F. Huxley. 1952. A quantitative description of membrane currents and its application to conduction and excitation in nerve. *J. Physiol. (Lond.).* 117:500–544.

Hoshi, T., W. N. Zagota, and R. W. Aldrich. 1990. Biophysical and molecular mechanisms of *Shaker* potassium channel inactivation. *Science.* 250:533–538.

Hoshi, T., W. N. Zagota, and R. W. Aldrich. 1991. Two types of inactivation in *Shaker* K^+ channels: effects of alterations in the carboxy-terminal region. *Neuron.* 7:547–556.

Isacoff, E. Y., Y. N. Jan, and L. Y. Jan. 1991. Putative receptor for the cytoplasmic inactivation gate in the *Shaker* K^+ channel. *Nature.* 353: 86–90.

Isom, L. L., K. S. De Jongh, and W. Catterall. 1994. Auxiliary subunits of voltage-gated ion channels. *Neuron.* 12:1183–1194.

Isom, L. L., K. S. De Jongh, D. E. Patton, B. F. X. Reber, J. Offord, H. Charbonneau, K. Walsh, A. L. Goldin, and W. A. Catterall. 1992. Primary structure and functional expression of the β_1 subunit of the rat brain sodium channel. *Science.* 256:839–842.

Levy, D. I., and C. Deutsch. 1996. A voltage-dependent role for K^+ in recovery from C-type inactivation. *Biophys. J.* 71:3157–3166.

Liss, L., J. LoTurco, and S. J. Korn. 1999. Contribution of the selectivity filter to inactivation in potassium channels. *Biophys. J.* 76:253–263.

Makielski, J. C., J. T. Limberis, S. Y. Chang, F. Zheng, and J. W. Kyle. 1996. Co-expression of β_1 with cardiac sodium channels decreases lidocaine block. *Mol. Pharmacol.* 49:30–39.

Makita, N., P. B. Bennett, and A. L. George. 1994. Voltage-gated Na^+ channels β_1 subunit mRNA expressed in adult human skeletal muscle, heart, and brain is encoded by a single gene. *J. Biol. Chem.* 269: 7571–7578.

Makita, N., P. B. Bennett, and A. L. George. 1996. Molecular determinants of β_1 subunit induced gating modulation in voltage-dependent Na^+ channels. *J. Neurosci.* 16:7117–7127.

Marban, E., T. Yamagishi, and G. Tomaselli. 1998. Structure and function of voltage-gated sodium channels. *J. Physiol. (Lond.).* 508.3:647–657.

McCormick, K. A., L. I. Isom, D. Ragsdale, D. Smith, T. Scheuer, and W. A. Catterall. 1998. Molecular determinants of Na^+ channel function in the extracellular domain of the β_1 subunit. *J. Biol. Chem.* 273: 3954–3962.

Nuss, H. B., N. Chiamvimonvat, M. T. Perez-Garcia, G. F. Tomaselli, and E. Marban. 1995. Functional association of the β_1 subunit with human cardiac (hH1) and rat skeletal muscle (μ1) sodium channel α subunits expressed in *Xenopus* oocytes. *J. Gen. Physiol.* 106:1171–1191.

O'Reilly, J. P., S. Y. Wang, R. G. Kallen, and G. K. Wang. 1999. Comparison of slow inactivation in human heart and rat skeletal muscle in Na^+ chimeras. *J. Physiol. (Lond.).* 515:61–73.

Patton, D. E., L. L. Isom, W. A. Catterall, and A. L. Goldin. 1994. The adult rat β_1 subunit modifies activation and inactivation gating of multiple sodium channels α subunit. *J. Biol. Chem.* 269:17649–17655.

Richmond, J. E., D. E. Featherstone, H. A. Hartmann, and P. C. Ruben. 1998. Slow inactivation in human cardiac sodium channels. *Biophys. J.* 74:2945–2952.

Rogart, R. B., L. L. Crebbs, L. K. Muglia, D. D. Kephart, and M. W. Kaiser. 1989. Molecular cloning of a putative tetrodotoxin-resistant rat heart Na^+ channel isoform. *Proc. Natl. Acad. Sci. USA.* 86:8170–8174.

Ruben, P. C., J. G. Starkus, and M. D. Rayner. 1992. Steady-state availability of sodium channels: interactions between activation and slow inactivation. *Biophys. J.* 61:941–955.

Rudy, B. 1978. Slow inactivation of the sodium conductance in squid giant axons. Pronase resistance. *J. Physiol. (Lond).* 283:1–21.

Ruff, R. L. 1996. Single-channel basis of slow inactivation of Na^+ channels in rat skeletal muscle. *Am. J. Physiol.* 271:C971–C981.

Ruff, R. L., L. Simoncini, and W. Stühmer. 1988. Slow sodium channel inactivation in mammalian muscle: a possible role in regulating excitability. *Muscle Nerve.* 11:502–510.

Salgado, V. L., J. Z. Yeh, and T. Narahashi. 1985. Voltage-dependent removal of sodium inactivation by *N*-bromoacetamide and pronase. *Biophys. J.* 47:567–571.

Sawczuk, A., R. K. Powers, and M. D. Binder. 1995. Spike frequency adaptation studied in hypoglossal motoneurons of the rat. *J. Neurophysiol.* 73:1799–1810.

Starkus, J. G., and P. Shrager. 1978. Modification of slow sodium inactivation in nerve after internal perfusion with trypsin. *Am. J. Physiol.* 4:C238–C244.

Todt, H., S. C. Dudley, J. K. Kyle, R. J. French, and H. Fozzard. 1999. Ultra-slow inactivation in μ1 Na^+ channels is produced by a structural rearrangement of outer vestibule. *Biophys. J.* 76:1335–1345.

Townsend, C., and R. Horn. 1997. Effect of alkali metal cations on slow inactivation of cardiac Na^+ channels. *J. Gen. Physiol.* 110:23–33.

Trimmer, J. S., S. S. Cooperman, S. A. Tomiko, J. Zhou, S. M. Crean, M. B. Boyle, R. G. Kallen, Z. Sheng, R. L. Barchi, F. J. Sigworth, R. H. Goodman, W. S. Agnew, and G. Mandel. 1989. Primary structure and functional expression of a mammalian skeletal muscle sodium channel. *Neuron.* 3:33–49.

Valenzuela, C., and P. B. Bennett. 1994. Gating of cardiac Na^+ channels in excised membrane patches after modification by α-chymotrypsin. *Biophys. J.* 67:161–171.

Vedantham, V., and S. C. Cannon. 1998. Slow inactivation does not affect movement of the fast inactivation gate in voltage-gated Na^+ channels. *J. Gen. Physiol.* 111:83–93.

Wang, S. Y., and G. K. Wang. 1997. A mutation in segment I-S6 alters slow inactivation of sodium channels. *Biophys. J.* 72:1633–1640.

West, J. W., D. E. Patton, T. Scheuer, Y. Wang, A. L. Goldin, and W. A. Catterall. 1992. A cluster of hydrophobic amino acid residues required for fast Na^+-channel inactivation. *Proc. Natl. Acad. Sci. USA.* 89: 10910–10914.

Yang, J. S., P. B. Bennett, N. Makita, A. L. George, and R. L. Barchi. 1993. Expression of the sodium channel β_1-subunit in rat skeletal muscle is selectively associated with the tetrodotoxin-sensitive α subunit isoform. *Neuron.* 11:915–922.